Journal of Alloys and Compounds 584 (2014) 494–502

Contents lists available at ScienceDirect

Journal of Alloys and Compounds

journal homepage: www.elsevier.com/locate/jalcom

Hot deformation behavior and hot working characteristic of Nickel-base electron beam weldments

Yongquan Ning [a,*], Zekun Yao [a], Hongzhen Guo [a], M.W. Fu [b]

[a] School of Materials Science and Engineering, Northwestern Polytechnical University, Xi'an 710072, PR China
[b] Department of Mechanical Engineering, The Hong Kong Polytechnic University, Hung Hom, Kowloon, Hong Kong, PR China

ARTICLE INFO

Article history:
Received 29 May 2013
Received in revised form 7 September 2013
Accepted 17 September 2013
Available online 25 September 2013

Keywords:
Nickel-base superalloys
Electron beam (EB) weldments
Hot deformation behavior
Hot working characteristic
Processing map

ABSTRACT

The electron beam welding (EBW) of Nickel-base superalloys was conducted, and the cylindrical compression specimens were machined from the central part of the electron beam (EB) weldments. The hot deformation behavior of EB weldments was investigated at the temperature of 960–1140 °C and the strain rate of 0.001–1.0 s^{-1}. The apparent activation energy of deformation was calculated to be 400 kJ/mol, and the constitutive equation that describes the flow stress as a function of strain rate and deformation temperature was proposed for modeling of the hot deformation process of EB weldments. The processing map approach was adopted to investigate the deformation mechanisms during the hot plastic deformation and to optimize the processing parameters of EB weldments. It is found that the true strain has a significant effect on the efficiency of power dissipation (η). The η value in the safe processing domain (1140 °C, 1.0 s^{-1}) increases from 0.32 to 0.55. In the unsafe processing domain (1080 °C, 0.001 s^{-1}), however, the η value greatly decreases with the increase of strain. When the strain is 0.40, the efficiency of power dissipation becomes negative. The flow instability is predicted to occur since the instability parameter $\xi(\dot{\varepsilon})$ becomes negative. The hot deformation of EB weldments can be carried out safely in the domain with the strain rate range of 0.1–1.0 s^{-1} and the temperature range of 960–1140 °C. When the height reduction is about 50%, the optimum processing condition is (T_{opi}: 1140 °C, $\dot{\varepsilon}_{opi}$: 1.0 s^{-1}) with the peak efficiency of 0.55 for the processing of EB weldments.

1. Introduction

Electron beam welding (EBW) is a fusion joining process with high density of energy in vacuum environment. The welds are usually produced without filler metal and the joints are obtained by the fusion of base metals. This technique is widely used in aerospace and nuclear industries for complex weld structures [1,2]. Recently, a great number of researches have been conducted to EBW techniques for metallic materials [3–5]. Rao et al. [3] investigated the reasons for superior mechanical and corrosion properties of aluminum alloy electron beam welds. Saresh et al. [4] explored and summarized the EBW process of Ti–6Al–4V alloy. Ferro et al. [5] studied EBW process for Inconel 706 and analyzed the influence of weld heat input on the microstructure of joint's zone. Generally, Ni-base superalloys are difficult to weld and suffer from the solidification cracking or/and the heat affected zone liquation cracking during welding in fusion zone. Vishwakarma et al. [6] investigated the microstructures developed in the fusion zone and the heat affected zone of the EB welded 718 Plus alloy. Fusion zone solidification cracking is caused by accommodating thermal and mechanical stresses during the final stages of solidification. Heat affected zone liquation cracking results from the formation of liquid film at grain boundaries during the weld-thermal cycle and the inability of this film to accommodate the thermally induced stresses during weld cooling [7]. Otherwise, the solidification in EBW is a nonequilibrium process. The formation of the nonequilibrium phases is generally detrimental due to the microcracking. They can become the crack sources that decrease stress rupture and tensile ductility, and lead to early failure of the EB weldments. To eliminate all the defects, the following hot working process including hot plastic deformation becomes a key process. Fig. 1 schematically illustrates the microstructure evolution in EB weldments after hot plastic deformation.

In the present study, the EBW of the mechanically polished Ni-base superalloys GH4133B was conducted. The cylindrical compression specimens were machined from the central part of the EB weldments. To investigate the effect of hot plastic deformation on the EB weldments, the isothermal compression tests of the above-mentioned cylindrical specimens were conducted. Based on the compression results and the related analyses, the flow behavior was investigated and the constitutive model established. In addition, the processing map approach was employed for exploration of the deformation mechanism during hot compression

* Corresponding author. Tel.: +86 29 88493744; fax: 86 29 88492642.
E-mail address: ningke521@163.com (Y. Ning).

0925-8388/$ - see front matter Crown Copyright © 2013 Published by Elsevier B.V. All rights reserved.
http://dx.doi.org/10.1016/j.jallcom.2013.09.112

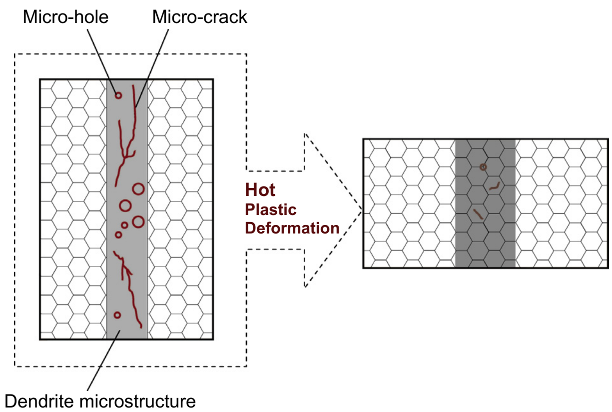

Fig. 1. Schematic illustration of the weldments after hot plastic deformation.

process and the optimization of the hot forging process of the EB weldments.

2. Material and experimental procedure

The nominal composition of GH4133B superalloy used in this work is: Cr, 20.0; Nb, 1.5; Ti, 2.5; Al, 1.0; Si, 0.30; Mn, 0.30; C, 0.03; B, 0.03; Ce, 0.01; Ni-bar. Fig. 2a shows a typically wrought microstructure of the as-received GH4133B superalloys with the grain size of 30–80 μm. The block specimens with the dimension of 30 mm × 30 mm × 6 mm were prepared by using the mechanical polishing of EBW. The mechanical polishing was performed in the following procedure: after the surface grinding with 30 μm grained diamond disk, the specimen was polished with a diamond paste of 18, 9 and 3 μm granulation for a few minutes. A polishing with a 0.1 μm colloidal silica solution was done for 30 min. The EBW was then conducted by using a KS55-G150 with an accelerating voltage of 150 kV. The electron current is 32 mA and the welding speed was selected as 2 mm/s. The cylindrical compression specimen with the dimension of ∅8 mm × 12 mm was machined from the central of the EB weldments. Fig. 2b obviously presents the fusion zone and the base metal in the cylindrical compression specimen, and Fig. 2c shows the dendrite microstructure in the fusion zone at higher magnification.

A series of isothermal compression tests were conducted by using a Gleebe-1500D thermo-simulation machine at the deformation temperature (T_d) of 960, 1020, 1080 and 1140 °C. The Temperature was controlled within ±2 °C. The strain rates ($\dot{\varepsilon}$) used are 0.001, 0.01, 0.1 and 1.0 s^{-1}, respectively, and the height reduction is 50%. All of the specimens were heated at a heating rate of 10 °C/s and soaked for 3.0 min at the deformation temperature to obtain a uniform temperature distribution in the entire specimen. The strain–stress curves were automatically recorded in the compression process. Upon compression, the specimens were cooled down to room temperature by spraying of water. The samples were sectioned parallel to the compression axis. The microstructure observations were conducted by using an OLYMPUS-PM3 optical microscope (OM) and the chemical etchant of $CuSO_4$ (10 g) + H_2O_2 (10 mL) + HCl (40 mL) + H_2O (50 mL) was used.

3. Experimental results and discussion

3.1. Flow behavior of Nickel-base electron beam weldments

To illustrate the deformation behavior of EB weldments, the true stress–strain curves at different temperatures under the strain rate of 1.0–0.001 s^{-1} are given in Fig. 3. The flow stress curve shows four different stages, viz., work hardening stage, stable stage, softening stage and steady stage. The flow stress exhibits an initial increase with strain until a peak stress value is established in the curve. After the peak stress, the stress decreases with the increase of strain. Under a low strain rate condition ($\dot{\varepsilon} = 0.001\ s^{-1}$), a steady stress state is achieved in which the flow stress remains nearly constant with the increasing strain. These flow stress–strain curves indicate that the softening mechanism, such as dynamic recrystallization, is sufficient to cancel out the work hardening effect. These results have a good agreement with the observations of wrought superalloy GH4133B [8] and Inconel superalloy 718 [9].

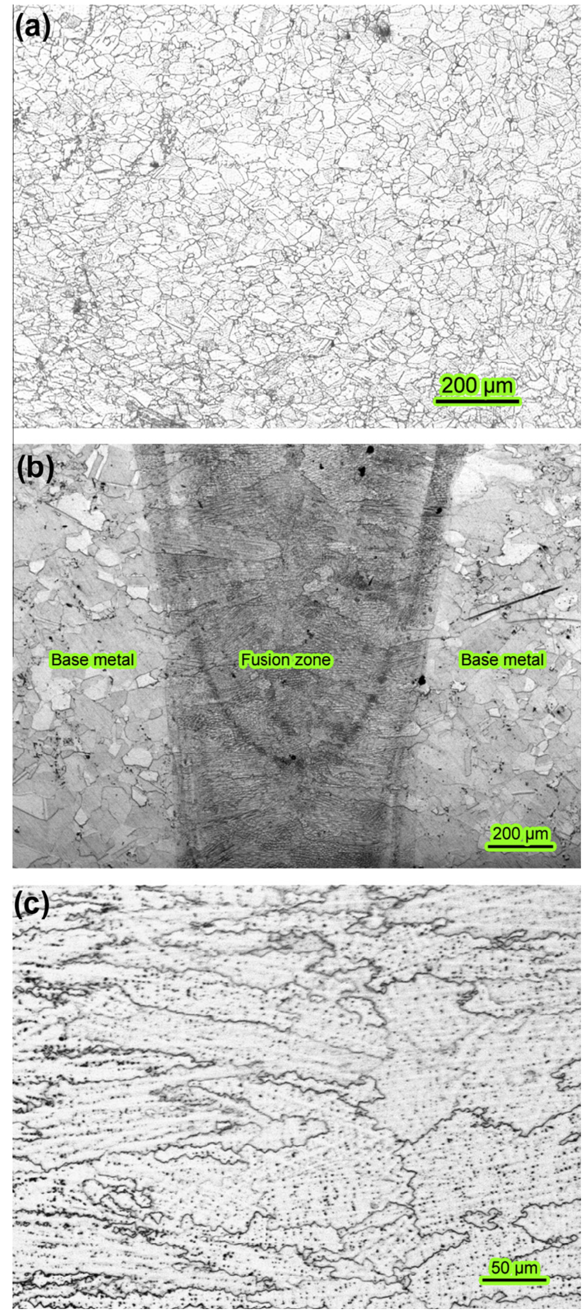

Fig. 2. Typical microstructures of the as-received GH4133B superalloy and its electron beam weldments. (a) Typical microstructure of the as-received superalloy. (b) Typical microstructure of the EB weldments. (c) Dendrite microstructure in fusion zone at higher magnification.

Furthermore, the peak stress values of the compressed EB weldments are observed. The peak stresses decrease with the increase of deformation temperature, whereas they all increase with strain rate. The effects of temperature and strain rate on the strain at peak stress suggest that this phenomenon is thermally activated. The flow softening behavior described above is a typical manifestation of the occurrence of dynamic recovery (DRV) and dynamic recrystallization (DRX). For the metals with low stacking fault energy like nickel and austenitic iron, climb and cross slip of dislocations tend to be hindered in the deformation process. The thermal activation is thus required for the plastic deformation of these metals. When a critical deformation condition is reached, DRX may take place instead of DRV. In addition, the peak stress has a small